The American Journal of Pathology, Vol. 181, No. 1, July 2012

http://dx.doi.org/10.1016/j.ajpath.2012.03.040

Vascular Biology, Atherosclerosis, and Endothelium Biology

Solid-Phase Immunoglobulins IgG and IgM Activate Macrophages with Solid-Phase IgM Acting via a Novel Scavenger Receptor A Pathway

Joseph J. Boyle,* Ivy Christou,† M. Bilal Iqbal,* Aivi T. Nguyen,* Viola W.Y. Leung,* Paul C. Evans,* Yu Liu,*‡ Michael Johns,* Paul Kirkham,‡ and Dorian O. Haskard*

From the Vascular Sciences Section and Pulmonary Pharmacology,‡ National Heart and Lung Institute, Imperial College London, London; and the Sir William Dunn School of Pathology,† University of Oxford, Oxford, United Kingdom*

IgG may accelerate atherosclerosis via ligation of proinflammatory Fcγ receptors; however, IgM is unable to ligate FcγR and is often considered vasculoprotective. IgM aggravates ischemia-reperfusion injury, and solid-phase deposits of pure IgM, as seen with IgM-secreting neoplasms, are well known clinically to provoke vascular inflammation. We therefore examined the molecular mechanisms by which immunoglobulins can aggravate vascular inflammation, such as in atherosclerosis. We compared the ability of fluid- and solid-phase immunoglobulins to activate macrophages. Solid-phase immunoglobulins initiated prothrombotic and proinflammatory functions in human macrophages, including NF-κB p65 activation, H_2O_2 secretion, macrophage-induced apoptosis, and tissue factor expression. Responses to solid-phase IgG (but not to IgM) were blocked by neutralizing antibodies to CD16 (FcγRIII), consistent with its known role. Macrophages from mice deficient in macrophage scavenger receptor A (SR-A; CD204) had absent IgM binding and no activation by solid-phase IgM. RNA interference–mediated knockdown of SR-A in human macrophages suppressed activation by solid-phase IgM. IgM binding to SR-A was demonstrated by both co-immunoprecipitation studies and the binding of fluorescently labeled IgM to SR-A-transfected cells. Immunoglobulins on solid-phase particles around macrophages were found in human plaques, increased in ruptured plaques compared with stable ones. These observations indicate that solid-phase IgM and IgG can activate macrophages and destabilize vulnerable plaques. Solid-phase IgM activates macrophages via a novel SR-A pathway. ***(Am J Pathol 2012, 181:347–361; http://dx.doi.org/10.1016/j.ajpath.2012.03.040)***

The role of immunoglobulins in atherosclerosis can vary with the context and stage of disease and with the isotype. In the case of IgM, we recently found that genetic prevention of secretion of serum IgM increased atherosclerotic lesion size more than threefold in low-density lipoprotein (LDL) receptor knockout mice mice, indicating that on balance IgM protects against early disease.[1]

Intriguingly, murine adoptive transfer experiments indicate that that B2 lymphocytes, which produce adaptive (somatically mutated, antigen-induced) IgG antibodies, promote atherosclerosis.[2] IgG, if immobilized on target cells by binding to surface antigens, can activate macrophages to kill the targets in one of the classic immunology phenomena, antibody-dependent cellular cytotoxicity. This is a major mechanism of autoimmune tissue damage in so-called type 2 hypersensitivity. It is well known that the low-affinity IgG receptor CD16 (*FCGR3*, FcγRIII) is selectively activated by more polymeric forms of IgG, such as solid-phase IgG or heat-aggregated (weakly cross-linked) IgG in fluid phase, conferring specificity for IgG bound to particles, normally pathogens.[3] We and others have shown that solid-phase IgG activates macrophages via CD16 in antibody-dependent cellular cytotoxicity,[3–5] and consistent with *in vivo* operation of this pathway, $CD16^{-/-}$ mice are protected from atherosclerosis on a low-density lipoprotein receptor knockout mice background.[6]

Supported by grants from the British Heart Foundation (FS/07/010 BHF Gerry Turner Intermediate Clinical Research Fellowship to J.J.B., a professorial award to D.O.H., and Programme award RG/03/009), by Hammersmith Hospitals Trustees Research Committee, and by the NIH Research Biomedical Research Centre funding scheme.

Accepted for publication March 20, 2012.

Supplemental material for this manuscript can be found at *http://ajp.amjpathol.org* or at *http://dx.doi.org/10.1016/j.ajpath.2012.03.040*.

Address reprint requests to Joseph J. Boyle, Ph.D., Vascular Sciences, NHLI, Imperial Centre for Experimental and Translational Medicine, Hammersmith Hospital, Du Cane Rd, London, UK W12 0NN. E-mail: joseph.boyle@imperial.ac.uk.

In contrast to the well-known homeostatic functions of IgM,[7] there are rare but illustrative clinical syndromes in which solid-phase deposits of pure IgM due to IgM-secreting plasma cell neoplasia provoke vascular inflammation characterized with a massive accumulation of $CD68^+$ macrophages (eg, cryoglobulinemic nephritis).[8] The existence of these diseases is proof of concept that solid-phase IgM in vessel walls can trigger vascular inflammation in humans *in vivo*. Similarly, in the mouse *in vivo*, IgM is known to amplify vascular injury in several models of ischemia-reperfusion injury, including in the coronary circulation, because of its capacity to activate complement.[9–12] Thus, it is entirely plausible that IgM, when in solid phase, plays a more pathogenic role in atherosclerosis than previously thought, akin to the accepted role of IgG.

Several protective mechanisms have been defined for IgM.[13] Binder et al[13] defined a role for IgM autoantibodies specific for epitopes on oxidatively modified low-density lipoproteins (oxLDLs). Notably, phosphorylcholine-reactive IgM natural (germline-encoded) antibodies are found in serum and atherosclerotic plaques and mediate antiatherogenic functions, such as inhibition of macrophage uptake of LDL cholesterol and foam cell formation.[13–15] This finding is corroborated by the atheroprotective effects of adoptive transfer of the B1a-lymphocyte subset that generates these antibodies[16] and our finding that $IgM^{-/-}$ accelerates atherosclerosis.[1] Because the IgG/CD16 pathway is already defined, in this article, we examine whether molecular mechanisms exist that would allow IgM to promote vascular inflammation and destabilize atherosclerotic plaques. We compared macrophage activation by IgG and IgM simply added to the culture supernatant (fluid phase) with that provoked by the same amounts of IgG and IgM preadsorbed to the tissue culture plastic (solid phase).

We found that, like IgG, solid-phase IgM activates macrophage functions linked to plaque instability, including H_2O_2-mediated killing of vascular smooth muscle cells (VSMCs) and expression of tissue factor (TF).[17,18] Solid-phase IgM was a stronger activator than solid-phase IgG, which was unexpected given the amount of data on IgG-mediated activation of leukocytes. Although macrophage activation by IgG was CD16 dependent, solid-phase IgM mediated macrophage activation by apparently analogous, novel low-affinity interactions with macrophage scavenger receptor A (SR-A; MSR1, CD204).[19] We found that there is an increase in immunoglobulin deposition in the vicinity of the lipid cores of coronary artery plaques in patients who had died of coronary disease when compared with plaques from noncardiac deaths. The capacity of solid-phase IgM and IgG to activate macrophages can therefore contribute significantly to the evolution of plaque rupture.

Materials and Methods

Reagents

Human IgM (The Binding Site, Birmingham, AL), human IgG (Sandoglobin, Sandoz, Frimley, UK), and bovine serum albumin (tissue culture grade; Sigma-Aldrich, Poole, UK) were purchased sterile and endotoxin free (manufacturer's assay) and diluted as required in sterile isotonic PBS (Sigma-Aldrich). Catalase (bovine liver catalase), pooled normal human serum, and C3-deficient serum were tissue culture grade (sterile, endotoxin tested) from Sigma-Aldrich. Dulbecco's modified Eagle's medium (DMEM) (Sigma-Aldrich) was phenol-red free to minimize background fluorescence. Avidin–fluorescein isothiocyanate (FITC) was from Sigma-Aldrich. Biotinylated albumin was from Abcam (Cambridge, UK). Biotinylated Fab fragments of anti-human IgM were from Abcam. The reactive oxygen species scavenger[20,21] *N*-acetyl-cysteine (Sigma-Aldrich) was dissolved in PBS at 0.1M, filter sterilized, and diluted as indicated to cultures. Uric acid (Sigma-Aldrich) was dissolved in PBS at 0.1M, filter sterilized, and diluted as indicated. Polyinosinic acid, polycytidylic acid, fucoidan allopurinol, dioctylcarbocyanine, *N*-acetyl-cysteine, and C3-deficient human serum were all from Sigma-Aldrich and were of the highest available grade, usually tissue culture grade, and were prepared aseptically, endotoxin tested, and filter sterilized. LDL was from Calbiochem (Beeston, England). Anti-CD16 (clones MEM-154 or LNK-16, which gave equivalent results; both from Abcam) and anti-CD64 (clone 10.1; IDS, Newcastle, UK) were functionally validated[22] in azide-free preparations at 1 $mg \cdot mL^{-1}$ and diluted to 10 $\mu g \cdot mL^{-1}$ final concentration and isotype controlled with mouse with IgG_1 (MOPC31C; Sigma-Aldrich) as previously detailed.[22]

Tissues and IHC

Tissues taken during autopsies of hospitalized patients who had died of myocardial infarction (MI) and causes unrelated to cardiovascular disease (control) had consent for use for research and UK Centre of Research Ethical Campaign approval. Their morphologic description has been previously published.[14] Human atherosclerotic plaques were formaldehyde fixed and paraffin embedded, and sections were deparaffinized, trypsinized for 20 minutes (IgM, IgG), or microwaved for 20 minutes (C4d, C3, C9, CD68) for antigen retrieval and then stained with unlabeled polyclonal antisera to IgM, IgG, C4d, C3, and C9 (all from Dako, Ely, UK) using a high-throughput robotic immunostainer (Menarini Diagnostics, Wokingham, UK) and visualized nonbiotinylated secondary detection system (Menarini) using peroxidase/diaminobenzidine. Double staining used the same antigen retrieval methods, where these were compatible, followed by manual staining, respective biotinylated secondary antisera (Dako), and detection with avidin-biotin-peroxidase (Dako) and Vector Red (Vector Laboratories, Peterborough, UK), or avidin-biotin-alkaline phosphatase (Dako) and Vector Blue (Vector Laboratories) as indicated.

Immunostaining Quantification

We examined culprit lesions from fatal MI cases, vulnerable lesions from the same case, and stable plaques from cases with a clear positive noncoronary cause of

death. Immunostaining strength is commonly assessed on a discrete 1+ to 3+ scale that is suitable for nonparametric analysis (eg, χ^2 test) but not for parametric methods (eg, analysis of variance). We extended the scoring concept to a 1- to 10-point continuous (nondiscrete) visual analog score scored by a masked observer. Each plaque had IgM immunostaining intensity scored on a 0- to 10-point continuous visual analog scale[23] (visual analog scales are robust in highly subjective estimates[23]). This procedure gave an IgM value for each donor. Gaussian distribution was checked with a stem-and-leaf plot. Then the arithmetic mean and SE were calculated for each group of patients (n = 10 MI cases, n = 16 non-MI controls) (significant difference, analysis of variance, $P < 10^{-5}$). There are two values for the MI patients: the ruptured and vulnerable plaques having been evaluated separately for each patient.

Computer-assisted image analysis was used to corroborate the visual analog scale score data by published methods.[24] Standardized low-magnification images of diaminobenzidine (brown)–stained sections [counterstained with hematoxylin (blue)] were captured as jpeg files and exported into ImageJ software version 1.44P (NIH, Bethesda, MD). The following operations were performed in Image J: RBG split, subtract red image from blue image, select region of interest, calculate histogram, and export data. We found that the RGB-split red image contained most of the brown coloring but also contained residual information from the blue-predominant hematoxylin dye and white areas. Subtracting the blue image made the pixel intensity brown specific. White areas have equal levels of red and blue, so they became zero. Hematoxylin staining areas had more blue than red, so they became negative on red-blue subtraction. The software automatically identifies negative values (light intensity cannot be <0) and redefines them as zero. Therefore, white becomes black, blue becomes black, and only red-brown becomes bright, which is then easily measured by intensity histograms. This gives an integral area of brown pixels, and the pixel intensity (brownness) is expressed as a semiquantitative measure of IgM density. The grayscale version of this method is already widely used to quantify Western blots. The IgM was quantified for each patient and expressed as mean ± SE for each group of patients.

Treatment of Tissue Culture Immunoglobulins

Accepted methods were used to polymerize immunoglobulins to reproducibly mimic immune complexes and bind them to culture plastic to reproducibly mimic tissue deposits. Serum samples were aseptically heat treated at 56°C for 30 minutes to destroy complement activity. Heat aggregation to polymerize immunoglobulins followed accepted methods; at 62°C ± 1°C (range) for 20 ± 1 minute (range), 96-well tissue culture plates (Nunclon surface; Nunc, Rochester, NY) were evenly coated by incubation with respective concentrations of antibody or control protein in 50 μL of PBS overnight in a tissue culture incubator. Coated plates were aseptically aspirated (with a disposable tip micropipette) and stored dry at 4°C for up to 1 month.

Co-Culture Cytotoxicity Assay

Most measurements of cell death were based on a 96-well plate assay that relies on release of a trapped intracellular fluorescent dye on cell death as previously described.[5,25] HCMED1-E6 VSMCs were grown in DMEM supplemented with 10% heat-treated fetal calf serum (FCS) (Sigma-Aldrich), penicillin, and streptomycin as before, trypsinized into suspension, washed twice in PBS, and then incubated in calcein-acetoxymethylester (Molecular Probes, Eugene, OR) in PBS adjusted to be both 1 μg/mL and 1 μg/10^6 cells in a tissue culture incubator for 20 minutes. Cells were then pelleted, washed once in standard medium and twice in PBS, counted, and added at 10^4 cells per well to a 96-well plate. Preliminary experiments indicated that HCMED1-E6 VSMCs labeled under these conditions showed a consistent linear relationship between cell number and fluorescence between 10^3 and 10^4 cells per well. Then U937 or human blood–derived macrophages were added at 10:1 U937 cells:VSMCs or 4:1 peripheral blood–derived macrophages:VSMCs. The cells were co-cultured in medium under the indicated conditions for 24 hours, the supernatant aspirated with a multichannel pipette, and the plates read either with a Tecan Spectrafluor Plus (Tecan, Reading, UK) or a Biotek Synergy HT (Potton, Bedfordshire, UK) using bottom optics, excitation (Ex) = 488 ± 10 nm, emission (Em) = 535 ± 10 nm, manual gain = 95 (Tecan), or automatic gain (Biotek), setting a high well (H12) containing 2×10^4 cells as 80,000 AFU. On the Tecan instrument, blank values were consistently approximately 1000 ± approximately 100 AFU with control readings consistently of 20,000 to 30,000 AFU. On the Biotek instrument, blank values were 5000 to 9000 AFU and control readings consistently 40,000 ± 1000 AFU. The Tecan instrument was used for most of the data with U937 macrophages (in a cell line only facility) and the Biotek for primary macrophages. Except where indicated, VSMC survival was calculated from the retained fluorescence:

$$\%\ \text{VSMC survival} = \frac{\text{well reading} - \text{blank}}{\text{Control VSMCs reading} - \text{blank}} \times 100\%$$

Flow Cytometry for Surface Binding

Cells were stained with annexin-V–FITC (Alexis; Enzo Life Sciences, Exeter, UK) for 20 minutes in binding buffer and counterstained with propidium iodide for 5 minutes. The necrosis controls were freeze-thawed three times in a −20°C freezer. For IgM binding studies, U937 cells were incubated with heat-aggregated IgM at 1 mg/mL for 20 minutes, washed once, and incubated with anti-human IgM and then with avidin-FITC. Cells were assessed unfixed using a Coulter EPICs XL flow cytometer (typically, 50,000 cells, FL-1 PMT voltage = 300; Beckman Coulter, Brea, CA) and appropriate forward scatter and side scatter gating excluded debris from the analysis.

IgM Coating of Beads

Microbeads chemically matched to the tissue culture surface (10-μm polystyrene, catalog number 17136, Polysciences, Eppelheim, Germany) were passively coated with IgM matched to the same density and same amount of IgM as for the activation experiments, under coating conditions matched to the well coating.

RNA Interference

Control (sc-37869) and SR-A–specific (sc-44116) RNA duplexes were purchased from Santa Cruz Biotechnology (Santa Cruz, CA) and reconstituted in 330 μL of sterile RNAase free deionized water to make a 10 μmol/L solution. Of this, 1 μL was mixed with 9 μL of Genlantis small-interfering RNA (siRNA) liposomes (AMS Biotechnology, Abingdon, UK) and left 20 minutes for complexes to form and then added to 10^5 U937 cells in 1 mL of DMEM without antibiotics or serum at 37°C for 8 hours (duplex concentration = 10 nmol/L). Then the cells were washed and added to the VSMC apoptosis assay, which was otherwise performed as described.

Western Blotting

A Novex XCell II (Invitrogen, Carlsbad, CA) minigel system was used throughout. U937 cells were dissolved in 10% SDS, heated to 100°C for 10 minutes., and then stored at −80°C. Proteins were separated by gel electrophoresis in 10% SDS, using precast 10% bis-Tris gels, 3-(*N*-morpholino)propanesulfonic acid buffer, and electrotransferred to polyvinylidene difluoride. Membranes were blocked with 4% nonfat milk protein in PBS 0.1% Tween-20 for 30 minutes, then stained with 1:5000 goat anti-CD204 (Abcam) for 24 hours at 4°C, developed with 1:5000 anti-goat peroxidase secondary (Dako), and visualized with ECL-Plus (Amersham, Amersham, UK), semilogarithmic exposure series (0.5, 2, 4, and 8 minutes) to Hyperfilm (Amersham) and X-O-Mat processor (Kodak, Cambridge, UK), according to the manufacturer's instructions. As a loading control, membranes were reprobed using anti-β-actin (Abcam ab8226) at 1:50,000 dilution, developed with anti-mouse peroxidase 1:10,000 (Dako) and visualized as for SR-A.

IgM Bead Precipitation Analysis

IgM-coated or control beads were added to U937 in 24-well plates, incubated for 20 minutes at 37°C, then harvested and dissolved in IP lysis buffer at 4°C for 20 minutes [composition: 10 mmol/L Tris-HCl, pH 7.6, 5 mmol/L EDTA, 50 mmol/L NaCl, 30 mmol/L sodium pyrophosphate, 50 mmol/L NaF, 100 μmol/L Na_3VO_4, and 1% Triton X-100; supplemented with protease inhibitors (5 mg/mL of aprotinin, 1 mmol/L pepstatin, 1 μg/mL of antipain, 1 ng/mL of leupeptin, and 100 mmol/L phenylmethylsulfonyl fluoride)]. In the bead precipitation experiments, the lysates were then centrifuged (13,000 × *g*, 5 minutes, Eppendorf 524 microfuge) and the pellets (ie, polystyrene beads, attached IgM, and any other attached proteins) collected and boiled in 10% SDS for 10 minutes. The SDS lysates from polystyrene beads were then immunoblotted for SR-A as described.

Turbimetric Clotting Assay

We made a minor adaptation of a validated one-step plasma recalcification time assay, using a 96-well plate to maximize throughput. Monocytes were isolated and cultured as described for 24 hours. After 24 hours, the supernatant was removed, with the cells remaining adherent to the base of the wells, and washed with PBS twice to remove any culture medium and serum. Then 100 μL of autologous citrated plasma was added to the wells and recalcified with 2 μL of 1.0M $CaCl_2$ to initiate clotting. The plates are immediately placed in a spectrophotometer (Synergy HT, Biotek) with internal thermostatic control at 37°C. Clotting was assessed as turbidity by measuring absorbance (A_{405}) every minute for 120 minutes.

Mouse Macrophages

To obtain bone marrow macrophages, mice were sacrificed, and both the femur and tibia were dissected out and flushed with PBS. Cells were then cultured in DMEM supplemented with antibiotics, L-Glu, 10% fetal calf serum, and 10% L929-conditioned medium (a source of macrophage colony-stimulating factor) (10 flasks per mouse). After 6 days, cells were harvested by scraping and counted and identical numbers added to assays. To obtain peritoneal exudate macrophages, mice were injected i.p. with 2% w/v Biogel (BioRad, Hemel Hempstead, UK) as previously described,[26] and peritoneal exudate cells were obtained by lavaging the peritoneal cavity with cold PBS and 2 mmol/L EDTA after 4 days. Cells were added to 24-well plate and washed gently in warm medium after 45 minutes to remove residual Biogel.

IgM Binding

Macrophages were resuspended at 10^6 cells per 100 μL of PBS containing 20 $\mu g \cdot ml^{-1}$ fluid-phase mouse IgM (M3795 monoclonal IgM, Sigma-Aldrich) that had been heat aggregated at 62°C for 20 minutes. After 20 minutes at 37°C, cells were spun and resuspended in 1:200 anti-mouse IgM-FITC (1140–2, Southern Biotech, Birmingham, AL). Cells were then washed once in 1 mL of PBS, fixed in 1% paraformaldehyde, and read on a flow cytometer (CyAN, Beckman-Coulter) within 60 minutes.

Griess Assay

Nitrite was measured by the Griess assay as previously described.[27] Solutions were made of 1% sulfanilamide (Sigma-Aldrich) in 30% acetic acid and 1% napthyl-ethylene-diamine (Sigma-Aldrich) in acetic acid. The two solutions were then mixed immediately before use and 100 μL of mix added to 100 μl culture supernatant. Absorbance was read to 540 nm after 10 minutes and com-

pared with a sodium nitrite (Sigma-Aldrich) calibration curve in control (cell-free) culture medium.

H_2O_2 Assay

Cells were incubated with 1 μmol/L dihydrodichloro-fluorescein-diacetate-chloromethylketone (DCFDA, H_2O_2 reporter dye; Molecular Probes, Invitrogen) for 20 minutes in PBS at 37°C. The cells were then added to a 96-well plate, containing wells that had been precoated with mouse 1 μg of IgM or bovine serum albumin (BSA). After 18 hours incubation, fluorescence was read on a multiplate fluorescence reader as described.

SR-A Transfection

SR-A green fluorescent protein (GFP) and control GFP plasmids were a kind gift from Professor Siamon Gordon (University of Oxford). HEK293 cells were grown under standard cell culture conditions in 10% FCS DMEM and detached by digestion with trypsin solution (59418C, Sigma-Aldrich), creating a cell suspension. Cells were then seeded at 10^4 cells per well on 8-well chambered coverslips (Nunc) or at 10^5 cells per well in 24-well plates (Costar). A total of 1 μg of plasmid was mixed with 1 μL of Lipofectamine 2000 (Life Technologies, Renfrew, UK) following manufacturer's instructions, and the complexes were then added to HEK cells in serum-free medium following manufacturer's instructions at 1 μg of plasmid/10^5 cells. After 2 hours, serum was replaced, and after 24 hours, wells were directly imaged (coverslips) or were harvested into suspension with cell dissociation medium (Sigma-Aldrich) for flow cytometry.

Time Lapse Confocal Microscopy

A Zeiss LSM510Meta microscope (Carl Zeiss AG, Jena, Germany) was used with a modification of a previous setup.[28,29] The microscope was time series enabled, was set to a combination of fluorescein detection (Ex = 488 nm, Em = 535 ± 20 nm, photomultiplier tube 800v) and differential inference contrast optics (differential interference contrast and fluorescence-equipped lenses, channel D), and had a live cell setup (Perspex head box, 37°C, 5% CO_2, 100% humidity).

Flow Cytometry of SR-A–Transfected Cells

SR-A-GFP or control GFP-transfected HEK cells were stained for flow cytometry in suspension using heat-aggregated IgM at 1 $mg \cdot ml^{-1}$ at 37°C for 20 minutes followed by anti-human IgM allophycocyanin at 4°C for 20 minutes. IgM binding to cells were read using FL3 on a Beckman Coulter CyAN flow cytometer and analyzed using WinMDI. The FL1 channel was used to indicate transfection efficiency, which was >90% for HEK cells.

Flow Cytometry of Human Plaques

Human autopsy aortic plaques were collected with consent of the next of kin, positive ethical board review (UK Centre of Research Ethical Campaign), and Human Tissue Authority registration. Plaques were stored at −80°C until analysis. Plaque cores were subjected to fine needle aspiration with a 2-mL syringe containing 2 mL of PBS and a fine (orange) needle. Collected material was stained with anti-human IgM-FITC (Abcam) or isotype for 20 minutes on ice, washed twice in PBS, and then analyzed on a Dako CyAN, using settings standard for macrophages but with a lowered forward scatter threshold to capture smaller debris fragments (based on the immunohistologic findings).

Results

Immunoglobulins Activate Macrophages More Potently When in Solid Phase Than When in Fluid Phase

We have previously shown that solid-phase IgG is more potent than fluid-phase IgG for activation of macrophage-mediated killing because of aggregation of the low-affinity IgG Fc-receptor CD16 (FcγRIII, *FCGR3* gene).[4,22] We first tested whether the distinction between solid-phase and fluid-phase immunoglobulin also applied to IgM. As an initial experiment, we compared the effect of solid-phase and fluid-phase IgM and IgG on the ability to activate macrophages to kill VSMCs, using a well characterized model system (see *Materials and Methods*). Solid-phase IgM provoked U937 cells (a monocytic cell line) to kill VSMCs, but the same amount of IgM in solution did not (Figure 1A). Solid-phase IgG also induced VSMC death in a dose-dependent manner but less potently than solid-phase IgM (Figure 1B). As a control, immunoglobulin-free BSA had minimal effect (Figure 1C). Because IgM is pentameric, the order of potency was calculated on the basis of both moles and micrograms, but IgM was more potent than IgG with either calculation (not shown). Because VSMCs were selectively prelabeled with calcein, this assay measures solely VSMC death. Culture of macrophages alone on solid-phase IgM did not affect their survival (not shown).

IgG Activates Macrophages via CD16

We have previously shown that solid-phase IgG activates macrophages via CD16, whether bound to target mesangial cells or to culture substrate.[22] We therefore addressed the receptor and effector mechanisms involved in killing of VSMCs. Solid-phase, IgG-stimulated, macrophage-induced VSMC killing was prevented by antagonistic antibodies to CD16, the low-affinity IgG receptor, but not by antagonistic antibodies to CD64, the high-affinity IgG receptor (see Supplemental Figure S1 at *http://ajp.amjpathol.org*). This finding is consistent with our own previous data with IgG-stimulated killing and assays of antibody-dependent cellular cytotoxicity and with the wider literature.[3,4,22] Macrophage-induced VSMC killing was variably and incompletely inhibited by neutralizing antibodies to CD32 (not shown).

We next studied the effector systems used by the IgG-activated macrophages to kill VSMCs. IgG-stimu-

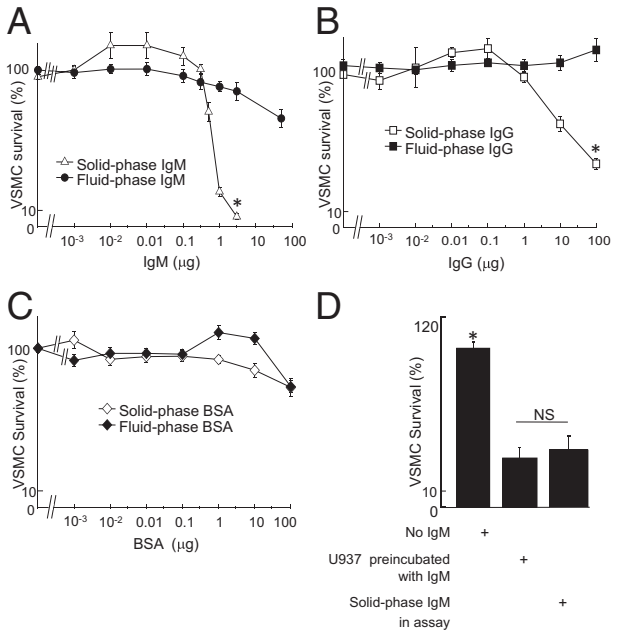

Figure 1. Solid-phase IgM and IgG activate U937 cells to kill VSMCs. U937 cells were incubated with IgM, either in solution or adsorbed to the plastic, and analyzed for cytotoxicity to VSMCs. **A-C:** VSMC survival in co-culture with U937 cells with IgM (**A**), IgG (**B**), or BSA (**C**), either solid phase or fluid phase. Values are mean ± SEM of five experiments; $^*P < 0.05$ by analysis of variance for indicated comparisons. **D:** Ability of IgM to induce VSMC killing in co-cultures is transferable via U937 cells preactivated by culturing on solid-phase IgM. U937 cells were added to wells coated with IgM for 4 hours, then transferred to IgM-free wells with VSMCs, and co-cultured for an additional 4 hours. NS, not significant. $^*P < 0.05$ by analysis of variance for indicated comparisons.

lated macrophage-induced VSMC death was unaffected by inhibitory antibodies to Fas ligand (FasL) or tumor necrosis factor (TNF)-α in concentrations that prevented killing by culture-matured macrophages.[30,31] Catalase, which selectively degrades H_2O_2, prevented IgG-stimulated macrophage-mediated killing of VSMCs (see Supplemental Figure S2 at *http://ajp.amjpathol.org*). Consistent with this, IgG stimulated macrophages to secrete H_2O_2 (see Supplemental Figure S3 at *http://ajp.amjpathol.org*).

Thus, solid-phase IgG activates macrophages via CD16 to kill co-cultured VSMCs, akin to the antibody-dependent cellular cytotoxicity–like activation that we have previously described,[4,22] which is consistent with CD16 as a low-affinity receptor for IgG. In contrast, we were highly intrigued by the IgM data because activating macrophages was not previously considered, and we therefore focused our efforts on dissecting this novel phenomenon.

IgM Activates Macrophages to Secrete H_2O_2

To test whether IgM evoked VSMC killing in co-cultures by activating macrophages or by sensitizing VSMCs, we then performed a transfer experiment. In this, co-cultures on IgM-coated plastic were compared with U937 cells that had been cultured on IgM-coated plastic and then transferred to separate cultures of VSMCs. U937 cells preincubated on IgM and then transferred to VSMCs on plastic produced as much killing as those incubated directly with both VSMCs and IgM in the assay (Figure 1D). Thus, VSMC death in the model was caused by IgM-induced macrophage activation.

Precoating of tissue culture plastic with IgM also consistently stimulated VSMC killing by fresh monocyte-derived macrophages (Figure 2A). This was fully inhibited by catalase and indeed reversed to a prosurvival effect, indicating involvement of hydrogen peroxide (Figure 2A). This also suggested, parenthetically, that IgM may initiate macrophage-derived survival responses that are normally masked by the strong proapoptotic effects of H_2O_2, but this was not a focus of the study. The concentration of H_2O_2 in supernatants of U937 cells cultured on IgM reached >100 μmol/L H_2O_2 (Figure 2B), which was at the top of the range at which VSMC killing was observed (10 to 100 μmol/L) (Figure 2C). The macrophage-activating effect of solid-phase IgM was inhibited by catalase in a concentration-dependent manner, with complete inhibition at 2000 IU $\cdot$ mL^{-1} (Figure 2D). In contrast, catalytically inactivated catalase had no effect (not shown). Because hydrogen peroxide can provoke either necrosis or apoptosis, we tested the mode of VSMC killing in our model by annexin-V and propidium iodide (PI) staining. In the first instance, we demonstrated that necrotic VSMCs (induced by freeze/thaw) were PI positive but annexin-V negative. Co-culturing macrophages with VSMCs on solid-phase IgM induced strong specific binding of fluorescent annexin-V to VSMCs, unaccompanied by PI positivity, indicating apoptosis (Figure 2E). In contrast, IgM did not induce annexin-V binding in cultures of VSMCs or macrophages alone. Adding catalase to parallel co-cultures on IgM prevented the development of annexin-V–positive VSMCs (Figure 2F). We also prelabeled VSMCs with the red fluorescent vital dye PKH26, added these to co-culture, and then double-stained with annexin-V–FITC. This indicated that the annexin-V–positive cells were red fluorescent labeled, indicating that they entirely derived from the prelabeled VSMCs (not shown). Thus, solid-phase IgM stimulates macrophages to induce VSMC apoptosis by releasing H_2O_2. The reactive oxygen species scavenger *N*-acetyl-cysteine also suppressed solid-phase IgM-stimulated macrophage-mediated killing in a concentration-dependent manner that was maximal at 1 mmol/L (see Supplemental Figure S4A at *http://ajp.amjpathol.org*). In addition, sensitivity of the IgM-activated killing to allopurinol, a specific inhibitor of the xanthine oxidase pathway of H_2O_2 secretion, indicated a role of the xanthine oxidase pathway in generating free radicals in this context (see Supplemental Figure S4B at *http://ajp.amjpathol.org*).

IgM in Solution Suppresses Macrophage oxLDL Uptake

Because a mouse natural monoclonal antibody has been shown to suppress macrophage oxLDL uptake and foam cell formation,[15] we repeated the experiment with whole human IgM. As expected, we found that whole human IgM in solution also suppressed foam cell formation (see

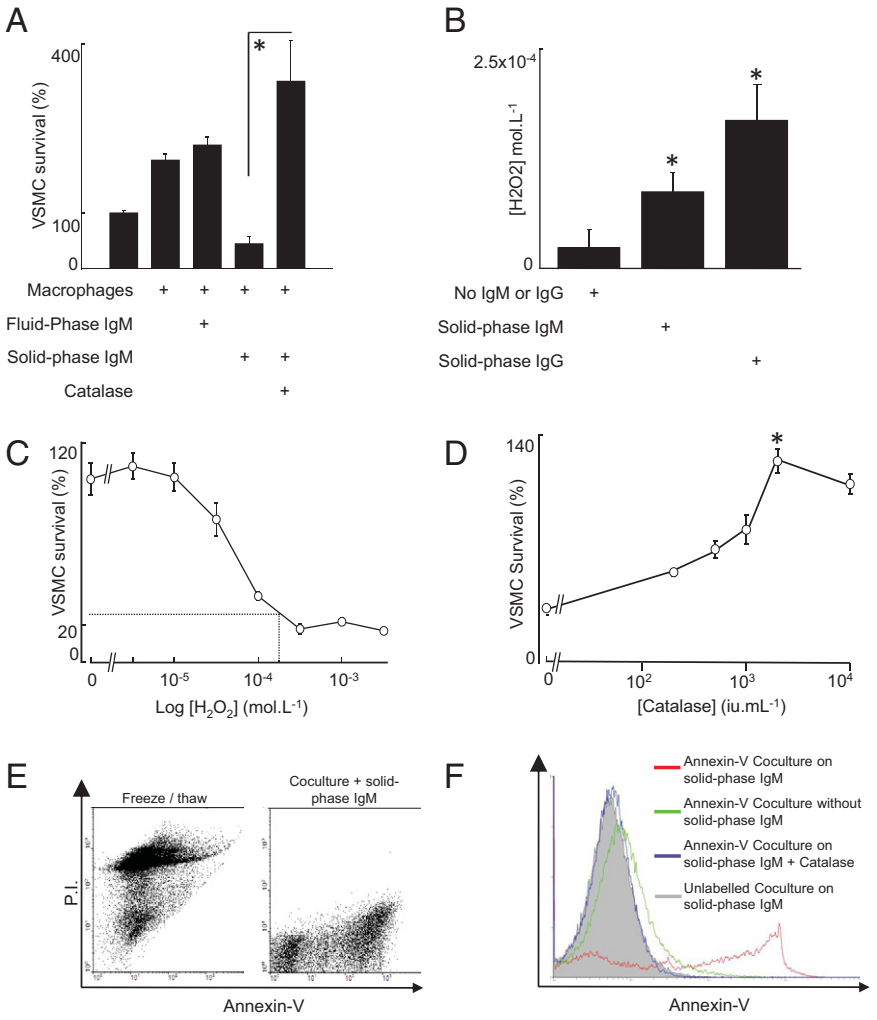

Figure 2. IgM-activated macrophages induce VSMC apoptosis via hydrogen peroxide. **A:** Human monocyte-derived macrophages were cultured for 24 hours on wells coated with 1 μg of IgM per well, after which VSMCs were added and their survival measured after a further 24 hours. Catalase (2000 IU $\times$ mL^{-1} of bovine liver catalase) reversed the cytotoxic effect of IgM-stimulated macrophages. **B:** U937 cells were incubated for 24 hours in untreated wells or wells with tissue culture plastic pretreated with IgG (100 μg per well) or IgM (1 μg per well), after which H_2O_2 was measured in supernatants by Amplex Red/Peroxidase (Molecular Probes); $^*P < 0.05$ by analysis of variance, Bonferroni adjusted with post hoc paired Student's *t*-test. **C:** VSMC viability, as measured by calcein release, after incubation with varying concentrations of H_2O_2 for 24 hours. The superimposed lines show that the concentration of H_2O_2 measured in the supernatant of U937 cells incubated with solid-phase IgM (100 μmol/L) induces 70% to 80% VSMC death. **D:** U937 cells and VSMCs were coincubated for 24 hours in wells pretreated with IgM (1 μg per well) with varying concentrations of catalase, after which VSMC viability was assessed. Data in **A-D** are mean $\pm$ SEM, $^*P < 0.05$, Student's *t*-test. **E:** Flow cytometric scatter plots showing that freeze thawing produces PI-bright, annexin-V–dim cells (indicative of necrosis). In contrast, co-culture of VSMCs with macrophages on solid-phase IgM produces annexin-V–bright, PI-negative cells, indicating apoptosis. The figure is representative of three separate experiments. **F:** VSMC cultures were incubated in the presence or absence of macrophages, IgM, and catalase and stained with annexin-V or control. Catalase blocked the development of the annexin-V positivity.

Supplemental Figure S5 at *http://ajp.amjpathol.org*), which is consistent with an atheroprotective role of IgM in fluid phase.

Solid-Phase IgM Enhances Macrophage Procoagulant Activity via TF

To address wider effects of IgM-mediated activation, we next assessed macrophage prothrombotic function in response to solid-phase IgM. We found that solid-phase IgM, but not fluid-phase IgM, increased macrophage procoagulant activity in a clot turbidity assay (Figure 3A). Stimulation of procoagulant activity by solid-phase IgM was associated with increased expression of TF mRNA (Figure 3B) and TF surface protein, with approximately 25% of macrophages becoming TF positive (Figure 3C).

Solid-Phase IgM Activates Macrophages via NF-κB

Contact with an IgM-coated surface activated NF-κB in U937 cells, evidenced by nuclear translocation of p65 NF-κB (Figure 4A). Moreover, MG132, a widely used inhibitor of NF-κB, suppressed IgM-activated macrophage killing of VSMCs (Figure 4B), although it increased killing stimulated by IgG (not shown). Further evidence supporting activation of NF-κB by solid-phase IgM came from inhibition of H_2O_2 production by BAY11-7082, a specific inhibitor of IKK2-mediated NF-κB activation[32] (Figure 4C).

Solid-Phase IgM Activates Macrophages Independently of Complement and Fc Receptor, Including CD16

We tested whether macrophage activation by IgM-coated culture surfaces requires complement. Heat inactivation or C3 deficiency of human serum in the culture medium made no difference to induction of VSMC killing by blood-derived macrophages cultured on IgM-precoated plastic (see Supplemental Figure S6A at *http://ajp.amjpathol.org*). A similar analysis of FCS showed that heat-inactivated and untreated FCS supported similar levels of macrophage cytotoxicity (see Supplemental Figure S6B at *http://ajp.amjpathol.org*). Moreover, killing was in fact increased in calcium-free PBS, excluding a signif-

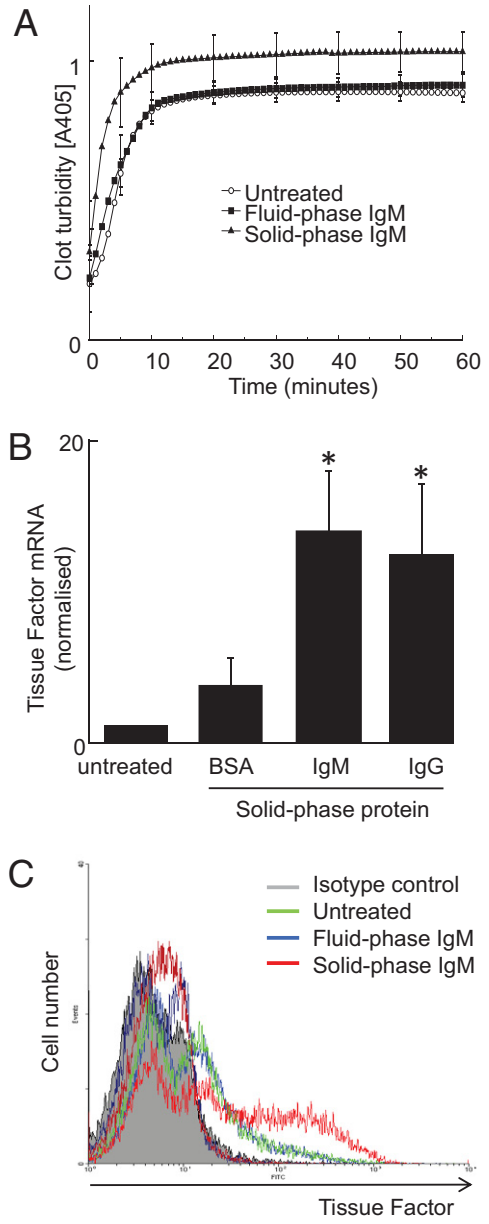

Figure 3. Solid-phase IgM but not IgM in solution activates human blood–derived macrophages to express TF. Human blood–derived macrophages were incubated with IgM, either in solution or adsorbed to the plastic, and analyzed for procoagulant activity and TF expression. **A:** Solid-phase IgM, but not fluid-phase IgM (10 μg $\times$ mL^{-1}), stimulates human blood–derived macrophage procoagulant activity, as measured using a clot turbidity assay. **B:** Cells were incubated with solid-phase IgM, IgG, or BSA (equal masses) for 24 hours and analyzed for TF mRNA using quantitative PCR. The *y* axis shows TF (f3, NCBI ccds: 53345.1) mRNA levels normalized to housekeeper (β-actin). Data are mean $\pm$ SEM; $^*P < 0.05$ by analysis of variance; $n = 5$. **C:** Cells were incubated with solid-phase IgM or fluid-phase IgM and analyzed by flow cytometry for surface TF protein, representative of at least three experiments using different donors.

icant role for macrophage-derived complement (see Supplemental Figure S6C at *http://ajp.amjpathol.org*). These data effectively exclude complement as an important modulator of macrophage cytotoxicity in response to solid-phase IgM in these experiments. Because macrophage activation by solid-phase IgG was prevented by antagonistic anti-CD16 antibodies, we studied whether the same was true of IgM. In contrast to IgG, neutralizing antibodies to CD16 had no effect on macrophage cytotoxic activation by solid-phase IgM (see Supplemental Figure S7 at *http://ajp.amjpathol.org*).

Enhanced Macrophage Activation by Heat-Aggregated IgM

We hypothesized that macrophage activation by solid-phase but not fluid-phase IgM may depend on an analogous low-affinity macrophage IgM receptor interaction analogous to IgG/CD16 binding (ie, capable of engaging polymeric but not monomeric IgM). We first examined CD16 itself by repeating the experiment in Supplemental Figure S1 for IgM. We found that antagonistic anti-CD16 antibodies have no inhibitory effect on IgM-induced macrophage activation (see Supplemental Figure S7 at *http://ajp.amjpathol.org*) and obtained similar negative data with anti-CD64 and anti-CD11b (not shown).

We therefore next sought to positively identify the (probable) low-affinity macrophage receptor for IgM. It is much more practicable to demonstrate binding of fluid-phase ligands using current technology, and we therefore used a high concentration of aggregated IgM as an experimentally tractable source of polymeric IgM. We were able to demonstrate by flow cytometry that heat-aggregated IgM, but not heat-aggregated BSA or monomeric IgM, bound to U937 cells in suspension (Figure 5A). Furthermore, heat-aggregated IgM further increased macrophage-induced VSMC killing when in solid phase

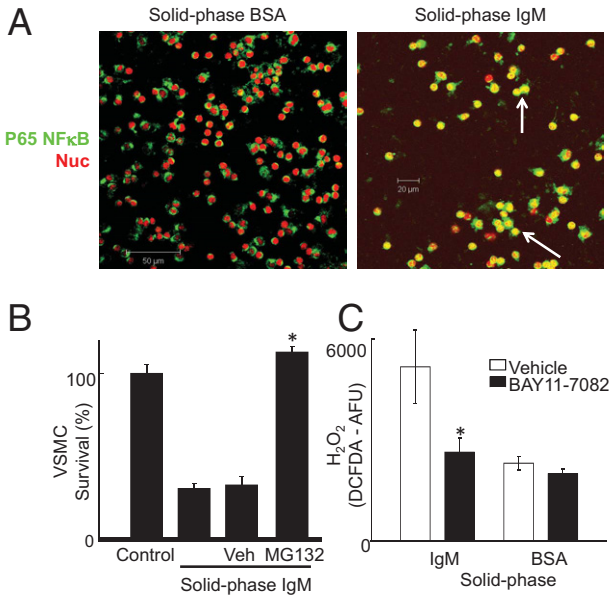

Figure 4. Solid-phase IgM activates macrophages via an NF-κB–dependent pathway. **A:** Confocal micrographs. Red indicates nuclear dye TOPRO-3; green, NF-κB p65 subunit immunofluorescence; and yellow, nuclear localization of NF-κB (examples indicated by **white arrows**). **B:** NF-κB inhibitor MG132 inhibits activation of macrophage killing of VSMCs by solid-phase IgM. U937 macrophages were preincubated with MG132 (50 μmol/L) for 20 minutes, washed in PBS, and then added to VSMC killing assays as before. $^*P < 0.05$, Student's *t*-test. **C:** BAY11-7082 (1 μmol/L), a specific inhibitor of IKK2-mediated NF-κB activation, was added to U937 macrophages at that start of incubation on surfaces with solid-phase IgM or BSA. H_2O_2 was measured by DCFDA fluorescence as before. $^*P < 0.05$, Student's *t*-test.

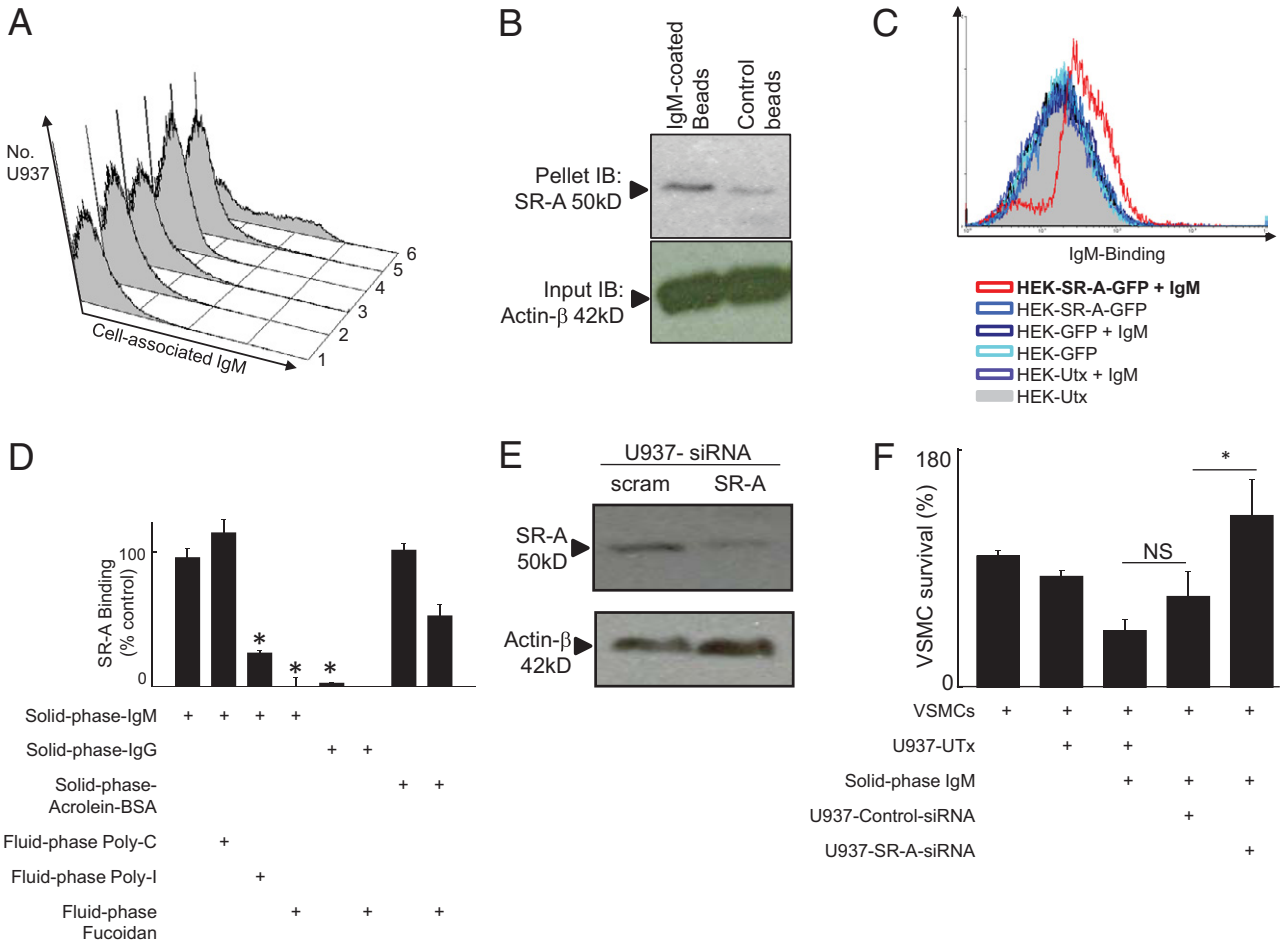

Figure 5. Solid-phase IgM binds and activates macrophages via SR-A. **A:** Fluid-phase IgM showed aggregation-dependent, temperature-dependent, selective surface binding to U937 cells. It is difficult to directly measure binding of solid-phase IgM to a cell surface, so we used aggregated fluid-phase IgM at a high concentration to probe binding to a suspected low-affinity receptor. Control or aggregated IgM in fluid phase (both at 1 mg · mL^{-1}) were incubated with U937 cells at 4°C or 37°C, after which binding was detected by flow cytometry using anti-IgM–FITC. (1) VSMCs incubated with aggregated BSA at 37°C; (2) VSMCs incubated with aggregated IgM at 37°C; (3) U937 cells incubated with aggregated BSA at 37°C; (4) U937 cells incubated with aggregated IgM at 4°C; (5) U937 cells incubated with monomeric IgM at 37°C; and (6) U937 cells incubated with aggregated IgM at 37°C. **B:** IgM surface-coated microbeads bind to SR-A in U937 cells. Western blotting with antibodies to SR-A or β-actin. Lanes 1 and 2, U937 cells were incubated at 37°C with polystyrene beads coated with IgM or uncoated. Control polystyrene microbeads pulled down a far smaller amount of SR-A (note, SR-A mediates adhesion to polystyrene). **C:** SR-A–GFP transfection confers IgM binding in HEK cells as detected by FITC-labeled anti-human IgM (Abcam, 1:100). UTx, untransfected. The *y* axis shows the cell number and the *x* axis fluorescence intensity. Histograms are colored as indicated. **D:** Recombinant purified Flag-tagged SR-A binds to IgM-coated plastic. The *y* axis shows binding of Flag-tagged SR-A to surfaces coated as indicated with either IgM, IgG, or acrolein-modified BSA (positive control). Poly-I, Poly-C (negative control competitor), or fucoidan was added at 500 μg · mL^{-1} as indicated. NS, not significant; $^{*}P < .05$, analysis of variance. **E:** SR-A–specific siRNA efficiently knocks down SR-A protein in U937 macrophages. Macrophages were treated for 18 hours with control or SR-A siRNA and protein lysate made in 10% SDS sample buffer. Control, nontargeting siRNA (Santa Cruz). SR-A, siRNA specific to SR-A (Santa Cruz). Immunoblots were developed (see *Materials and Methods*) with bands at appropriate M_r as indicated. Actin, loading control. **F:** SR-A knockdown reverses activation of macrophage killing of VSMCs by solid-phase IgM. Macrophages were either untransfected U937 (U937-UT) or U937 cells transfected with either control-siRNA (U937-control-siRNA) or SR-A-specific siRNA (U937-SR-A-siRNA). The *y* axis shows VSMC survival, as measured previously.

and evoked slight macrophage-induced VSMC killing in fluid phase at high concentrations (1 mg · mL^{-1}) (see Supplemental Figure S8A at *http://ajp.amjpathol.org*). We then performed an experiment in which the addition of IgM-coated beads was compared with IgM coating of the tissue culture plastic and found that these also stimulated macrophage reactive oxygen species secretion (see Supplemental Figure S8B at *http://ajp.amjpathol.org*).

Role of Macrophage SR-A

Because both SR-A and IgM mediate clearance of oxidized lipids, it was easy to imagine that ancient evolutionary pressures to optimize clearance of oxidized lipids might have driven cooperativity between the SR-A and IgM pathways. We hypothesized that macrophage activation by solid-phase IgM was mediated by SR-A. This was first tested using fluid-phase competitor ligands, which were reasoned to fill up receptor sites without causing aggregation-dependent activation. Fucoidan and polyinosinic acid (Poly-I), both macromolecular SR-A ligands, suppressed IgM-stimulated macrophage-induced VSMC death in a concentration-dependent manner. Polycytidylic acid (Poly-C), a control devoid of SR-A binding, actually reduced VSMC survival (see Supplemental Figure S9 at *http://ajp.amjpathol.org*). In contrast, IgG-stimulated macrophage-induced VSMC death was unaffected by fucoidan (see Supplemental Figure S10 at

http://ajp.amjpathol.org), which is consistent with its mediation by CD16 in Supplemental Figure S1 at *http://ajp.amjpathol.org*.

Supported by this pilot inhibition experiment, we performed co-precipitation studies. IgM bound to polystyrene beads pulled down SR-A from live macrophages when incubated at 37°C, indicating that SR-A binds to solid-phase IgM in live cells (Figure 5B). Moreover, we were able to demonstrate by flow cytometry that HEK cells transfected with SR-A–GFP bound fluorescently labeled aggregated IgM, whereas control HEK cells transfected with GFP did not (Figure 5C). Lastly, flag-tagged recombinant SR-A bound to plates coated with IgM but not to plates coated with IgG, and this binding was competitively inhibited by Poly-I and fucoidan but not by Poly-C (Figure 5D).

To obtain more specific evidence that SR-A mediated activation of macrophages by solid-phase IgM, we used an siRNA approach. We found that SR-A–specific siRNA suppressed SR-A protein level by >50% as assessed by Western blotting (Figure 5E) and abolished the ability of U937 macrophages to kill VSMCs in response to IgM (Figure 5F).

We explored the effect of solid-phase IgM on SR-A aggregation. We transfected HEK cells with GFP-tagged SR-A or control GFP plasmid and then added polystyrene beads. These beads aggregated most cellular SR-A, provided they were coated with IgM (Figure 6).

Lastly, to further substantiate our conclusion that SR-A mediates IgM binding and macrophage activation, we used SR-A$^{-/-}$ mice. Data are shown for bone marrow–derived macrophages (BMDMs) (Figure 7), although we obtained similar results using peritoneal exudate macrophages (not shown). Fluid-phase heat-aggregated IgM bound to the surface of wild-type (WT) macrophages, but SR-A$^{-/-}$ macrophages almost completely lacked IgM binding (Figure 7A). Performing incubation with IgM at 4°C abolished binding to WT macrophages (not shown). Solid-phase IgM induced NF-κB p65 nuclear translocation, secretion of NO-derived nitrite, and release of H_2O_2 in WT macrophages but not in SR-A$^{-/-}$ macrophages (Figure 7, B–D). Taken together, these data indicate that solid-phase IgM activates human and mouse macrophage via SR-A aggregation and NF-κB activation.

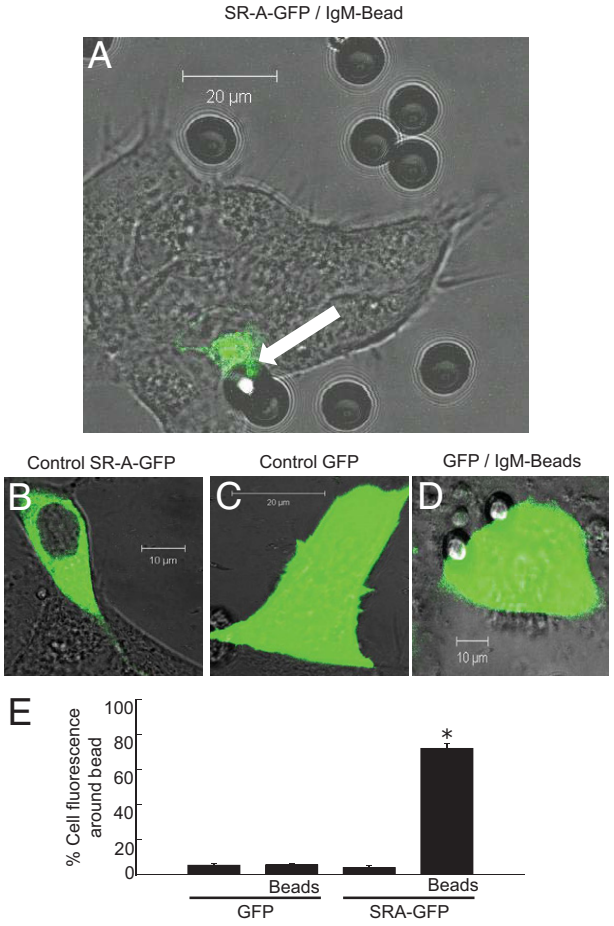

Figure 6. Cellular SR-A is aggregated by solid-phase IgM. HEK cells were transfected with plasmid for GFP or for GFP-tagged SR-A (gift, S. Gordon; see *Materials and Methods*). After 24 hours, the transfected HEK cells were imaged live in real time by confocal microscopy. **A:** SR-A–GFP–transfected cells, IgM-coated bead. **B:** SR-A–GFP–transfected cells, control. **C:** GFP-transfected cells. **Arrow**, aggregation of SR-A–GFP chimeric receptors at the contact with the IgM-coated bead. Representative of $n = 3$ transfections. **D:** GFP-transfected cells incubated with (and in contact with) IgM-coated beads. **E:** Statistical evaluation of aggregation in line with methods published for immunologic synapses. Data represent 100 cells from five transfections and are mean ± SE. The percentage of GFP fluorescence around (within 10 μm of) the bead was calculated (y axis) for cells transfected with GFP or with SR-A–GFP and incubated with IgM-coated beads as indicated. *$P < 0.05$, analysis of variance.

Vulnerable and Ruptured Plaques Are Characterized by Increased Particulate Solid-Phase IgM Around Macrophages in the Lipid Core

We assessed the distribution of IgM, IgG, and macrophages in coronary atherosclerotic plaques from a consecutive autopsy series.[6] IgM was highly abundant in the lipid cores of disrupted and vulnerable plaques from fatal myocardial infarction cases but not in plaques from control autopsy cases (ie, noncardiac deaths) (Figure 8). The excess IgM in ruptured plaques was specifically found in the lipid core (Figure 8, A and B), where it was identified coating solid-phase debris particles (Figure 8C), and was intimately associated with CD68$^+$ macrophage foam cells (Figure 8D). IgM immunostaining was scanty at other sites (Figure 8, A and B). The lipid core area of the plaque was consistently deficient in VSMC, a feature consistent with macrophage-induced VSMC apoptosis (not shown and widely described[33–36]). Plaques from control autopsy cases had relatively weak staining for IgM under the same conditions (Figure 8E). To test whether plaque IgM was surface bound, lipid core debris was recovered from advanced aortic plaques and surface stained with anti-IgM for flow cytometry. We found particulate debris in the plaque core, ranging from approximately 1 to 10 μm (not shown) and with significant surface-bound IgM (Figure 8F). Thus, plaques contain solid-phase immunoglobulins, indicating that the key aspect of the *in vitro* models indeed reflects human plaque cores. There was also IgG within plaques (Supplemental Figure S11, A–H at *http://ajp.amjpathol.org*),

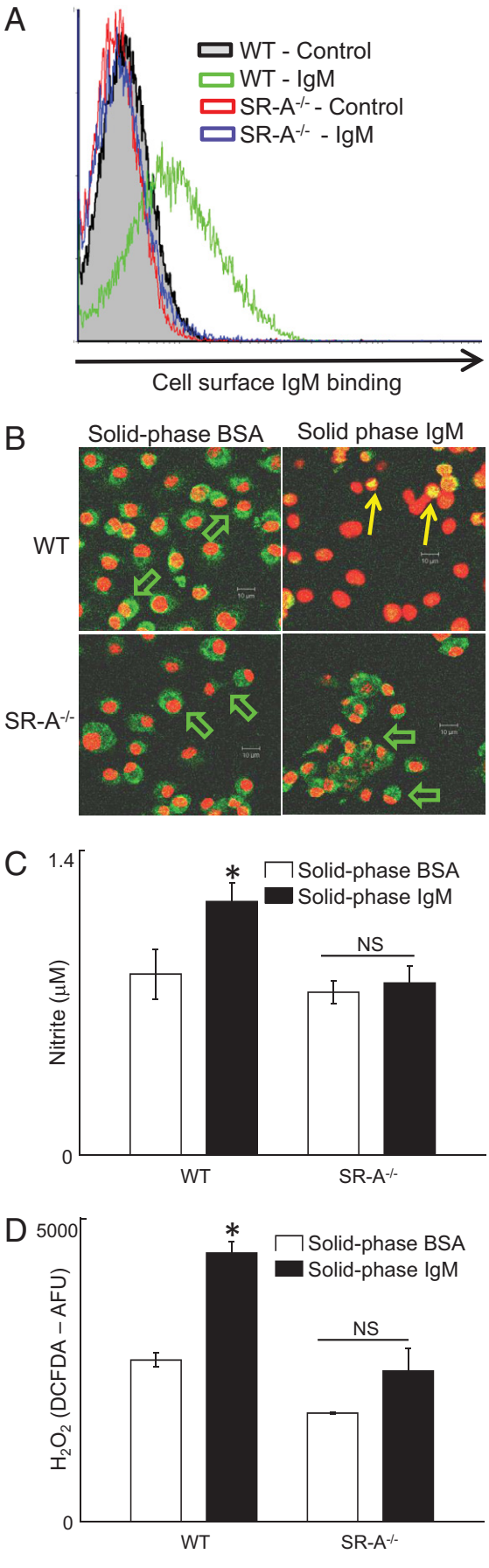

also in a solid-phase (particulate) distribution in the lipid necrotic core, as well as more diffuse staining consistent with its smaller size.[6]

Finally, we systematically evaluated immunoglobulins in ruptured lesions, distant unruptured coronary lesions ("vulnerable lesions") in patients with ruptured plaques, and coronary plaques from noncardiac death autopsies using a visual analog scale. This evaluation revealed considerably more IgM in ruptured plaques and in vulnerable lesions from the same cases as the ruptured plaques (n = 10 patients) than in coronary plaques from noncardiac deaths (n = 16 patients) (Figure 8G). Reanalysis with computer-aided image densitometry corroborated that there was more IgM in ruptured plaques than in plaques from control autopsies (Figure 8H).

Discussion

Our study provides a novel insight into the role of immunoglobulins in coronary artery disease and suggests that IgM and IgG might contribute to plaque instability. Although immunoglobulins in solution can protect macrophages from uptake of oxLDLs, once bound to a surface immunoglobulins activate macrophages to express procoagulant activity in the form of TF and to kill VSMCs by releasing H_2O_2 (and also NO in the case of IgG). Moreover, we have determined an entirely novel mechanism for macrophage activation by solid-phase IgM via recognition by macrophage SR-A.[37] This finding is a substantive advance to our understanding of immunoglobulin-macrophage interactions.

We have previously shown that deletion of secretory IgM accelerates atherosclerosis in early lesions in the mouse. Serum IgM comprises 30% of germline encoded T-independent natural antibodies derived from B1 lymphocytes and recognize anionic organic debris,[38] including phosphorylcholine in oxidatively modified LDLs and apoptotic cells.[38] The remainder of serum IgM comprises classic rearranged T-dependent adaptive antibodies de-

Figure 7. IgM binds to and activates macrophages from WT but not SR-A$^{-/-}$ mice. Bone marrow macrophages and peritoneal exudates macrophages were cultured from WT or SR-A$^{-/-}$ mice as described (n = 5 SR-A$^{-/-}$ mice, n = 5 WT mice). **A:** BMDMs were incubated with 20 $\mu g \cdot mL^{-1}$ heat-aggregated murine purified monoclonal IgM (Sigma-Aldrich) at 37°C for 20 minutes, washed briefly, then incubated with anti-mouse IgM FITC 20 minutes. The x axis shows FITC fluorescence (FL-1) and the y axis cell count. Representative of n = 5 mice of each strain and of BMDMs and peritoneal exudate cells. **B:** BMDMs were added to chamber slides (Labtek-I, Nunc) precoated with either BSA or mouse IgM, 0.03 $\mu g \cdot mm^{-2}$ (to match the other assays) for 30 minutes at 37°C, fixed in acetone, stained with anti-p65 NF-κB (sc8008, Santa Cruz) and counterstained with a nuclear dye (TOPRO), and then imaged by confocal. Green indicates p65 NF-κB; red, nuclei. **Green arrows** indicate cytoplasmic NF-κB in WT BMDMs on BSA and on SR-A$^{-/-}$ BMDMs on either IgM or BSA. **Yellow arrows** indicate nuclear localization of p65 NF-κB in WT BMDMs on IgM-coated surface. Scale bars indicate distances (all at the same magnification). **C:** The y axis shows nitrite in supernatant after 24 cultures on surface indicated. Open bars, 1 μg per well of BSA-coated surface; filled bars, 1 μg of IgM-coated surface; SR-A$^{-/-}$, supernatant from SR-A$^{-/-}$ BMDMs; and WT, supernatant from WT C57BL/6 BMDM. Cells were at 10^5 cell per well (cpw). *$P < 0.05$, paired Student's t-test. NS, not significant. **D:** H_2O_2 secretion. The y axis shows fluorescence from DCFDA, a H_2O_2-reporter dye after 18 hours. Open bars, 1 μg per well of BSA-coated surface; filled bars, 1 μg of IgM-coated surface. *$P < 0.05$, paired Student's t-test. NS, not significant.

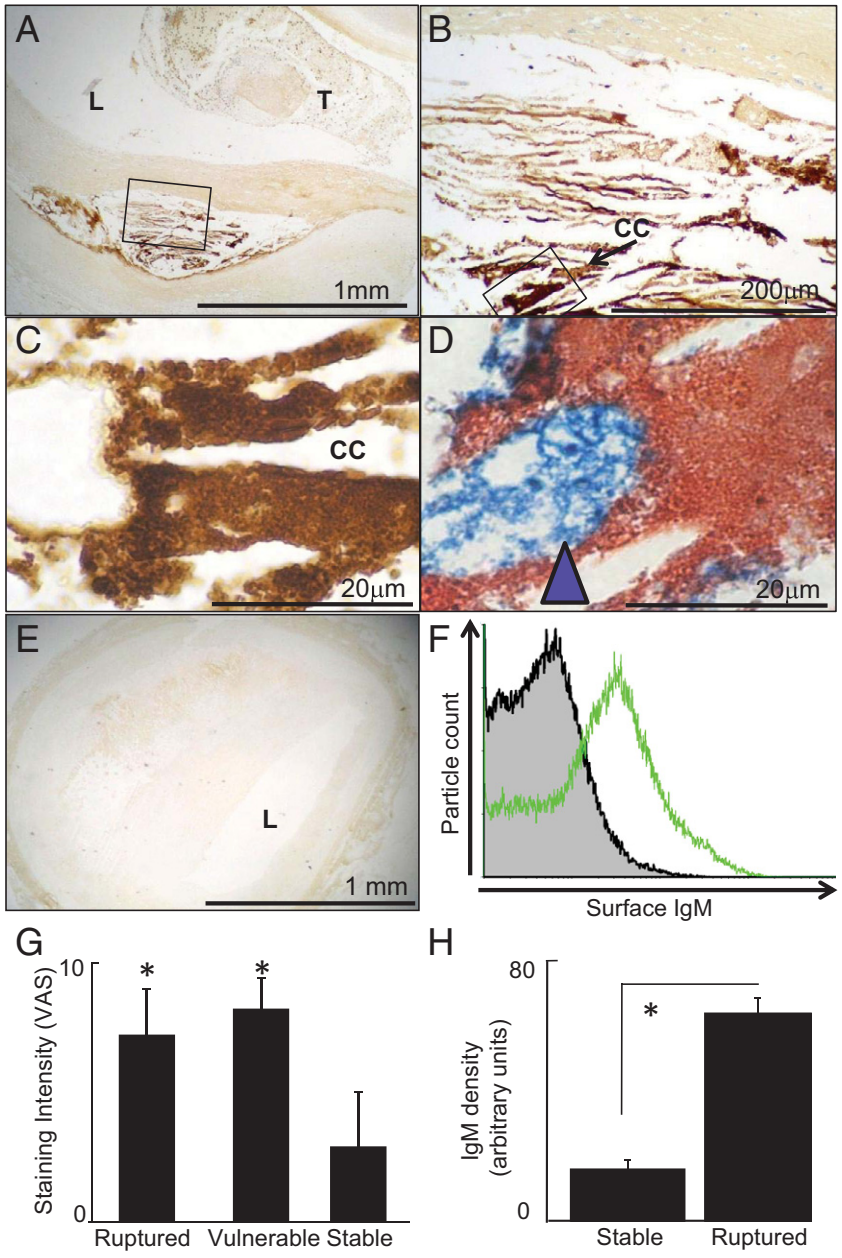

Figure 8. Ruptured plaques and vulnerable lesions contain IgM in contact with macrophages. Immunostaining for IgM was conducted on coronary atherosclerotic lesions responsible for coronary thrombosis and cardiac death (ruptured plaques) in comparison with unruptured coronary lesions from the same patients (vulnerable lesions) and coronary lesions from patients who had died of noncardiac causes (stable lesions). Scale bars indicate distances. Ruptured lesions have increased IgM deposits coating lipid core debris. **A-C:** Photomicrographs at successive magnifications of a representative culprit plaque immunostained for IgM; brown, positive immunopositivity; blue, nuclei; T, thrombus; L, lumen; CC, example cholesterol cleft. **B**: High power of box in **A**. **C:** High power of box in **B**; IgM covers granular lipid core debris structures. **D:** Representative micrograph of lipid core of ruptured plaques double-immunostained for IgM (red) and CD68 (blue). IgM-positive lipid core debris (red) is in intimate contact with macrophages (**blue arrowhead**). **E:** Representative micrograph of (unruptured) plaque from an autopsy with death due to a noncardiac cause, immunostained for IgM along with the ruptured plaque shown in A. **F:** Flow cytometry of plaque debris recovered from an advanced (calcified and slightly ulcerated) aortic plaque, representative of $n = 3$. The x axis shows surface IgM staining and the y axis particle number. Shaded gray histogram, isotype control. Open green histogram, anti-IgM–FITC. **G:** Ruptured plaques and vulnerable lesions have consistently more IgM than stable lesions. We examined culprit lesions from fatal MI cases, vulnerable lesions from the same case, and stable plaques from cases with a clear positive noncoronary cause of death. Each plaque had IgM immunostaining intensity scored on a 0- to 10-point continuous visual analog scale. This is a conceptual extension of the common 0, 1, 2, 3 scale to validly allow parametric data methods. Gaussian distribution was checked with a stem-and-leaf plot. The mean and SE were determined for each group of patients ($n = 10$ MI cases, $n = 16$ non-MI controls); $^*P < 10^{-5}$, significant difference, analysis of variance. **H:** We then performed a focused corroborative reanalysis of IgM in ruptured lesions in MI cases and stable lesions in non-MI controls using computer-aided morphometry as previously described.[24] The area of brown pixels and the pixel intensity brownness were integrated to express a semiquantitative measure of IgM density, along the lines of Western blot quantification. The IgM was quantified for each patient and expressed as mean ± SE for each group of patients. Ruptured plaques have increased IgM ($^*P < 10^{-5}$, Student's *t*-test) using this method.

rived from B2 cells that recognize specific neoepitopes or foreign epitopes jointly with CD4 T-helper cells.[2,7] Critically, although adoptive transfer of B1 cells is atheroprotective,[16] adoptive transfer of B2 cells is atheroaccelerant.[2] Taken together, these data suggest that the effects of immunoglobulins might be more complex than previously suspected.

Data on the role of SR-A in atherosclerosis *in vivo* have also been conflicting, with reports of strong proatherogenic effects, weak proatherogenic effects, antiatherogenic effects, and overall no effect.[19,39,40] In part, this is likely to reflect multifunctionality of SR-A.[19] However, the occurrence of plaque rupture in mouse models is controversial, and mouse models are unlikely to represent the biology of the unstable complex plaque that we have observed immunocytochemically in human lesions. Our mechanistic dissection of its role as a proinflammatory IgM receptor in advanced lesions may go some way to reconciling these data.

Multiple lines of evidence shown here link solid-phase IgM-mediated SR-A ligation to macrophage activation. With human cells, siRNA knockdown and direct binding assays indicated that solid phase or high concentrations of fluid phase aggregated IgM activate macrophages. Importantly, we also found that macrophages from SR-$A^{-/-}$ mice did not bind and were not activated by solid-phase IgM. Taken together, these data therefore indicate that the interaction between macrophages and solid-phase IgM is via SR-A in both humans and mice. We have not directly measured the affinity of this interaction but predict that it is low, thereby explaining the failure of monomeric IgM in solution to bind macrophages. In-

stead, we suggest that the high avidity invoked by aggregated or surface-attached IgM initiates SR-A receptor clustering, signaling, and the activation of macrophage effector functions, such as TF gene expression and H_2O_2 release. Indeed, we have previously shown that some solid-phase SR-A ligands activate macrophages.[41] Alternatively, solid-phase IgM, which is known to interact with the collagenous domain of C1q, could interact with the collagenous domain of SR-A and modify its conformation.[42] The former mechanism has a precedent in FcγR3/CD16 interactions with IgG[3] and in TNF superfamily members interacting with TNF receptor superfamily members.[43] Moreover, we found evidence of whole-cell SR-A aggregation by live cell microscopy. Related mechanisms are found in macrophage activation by so-called frustrated phagocytosis of solid-phase immune complexes,[44] possibly involving classical Fc-receptor signaling via tyrosine kinases.[3]

Our observation that solid-phase immunoglobulins activate macrophages adds to the growing body of work on the contribution of macrophages to plaque instability. We frequently used vascular smooth muscle cell apoptosis as a readout because of the role of VSMC apoptosis in plaque instability. Unstable plaques are characterized by increased macrophages, reduced collagen, and fewer VSMCs.[45] VSMCs are the only plaque cell types that synthesize structurally key collagen isoforms collagen I and collagen III.[45] Macrophages directly degrade collagen via matrix metalloproteinases.[33] We and others have found that macrophages also induce VSMC apoptosis, via Fas-L/Fas interactions, TNF, and NO, consequently preventing collagen synthesis.[30,46,47]

The pathophysiologic relevance of our *in vitro* experiments was strongly supported by the immunohistologic observation that immunoglobulins accumulate on necrotic core debris in the vicinity of macrophages in plaques of coronary arteries of patients who had died of coronary disease. This finding was corroborated by the flow cytometric observation that immunoglobulins are bound to the surface of lipid core particles, indicating that plaque IgM is in solid phase, similar to the *in vitro* stimulation. Hansson et al[48–51] seminally documented immunofluorescence for IgG and complement C3 in human and rabbit lesions associated with injured endothelial cells. In this study, we focused on mechanisms related to macrophages and plaque rupture and inferred that ruptured lesions contain far more IgM than do stable ones. Notably, plaque IgM was also increased in the intact coronary lesions separate from ruptured plaques of these patients, suggesting that it is a consequence of a generalized process in the "vulnerable patient"[35,52] and indicating that IgM deposition antecedes full plaque rupture. Although the exact mechanism of immunoglobulin entry is beyond the scope of the current article, there is evidence of potential mechanisms supporting entry of large molecules, such as IgM, to vulnerable plaques in humans. Ruptured plaques often have evidence of biological response to recent intraplaque hemorrhage, which could inject IgM into the plaque interior.[24] In contrast, IgG, which is smaller and more easily diffuses into tissues, had a wide diffuse pattern of distribution, in addition to lipid core particulate deposits, and was not obviously increased in ruptured plaques relative to stable (not shown). Findings with therapeutically aspirated thrombus indicate that subclinical plaque disruption and thrombosis frequently precede the clinically evident full rupture event,[53] which could also plausibly allow plasma easy access to the lesion interior.

Our findings call for a new look at whether IgM is solely protective in atherosclerosis.[1] Thus, fluid-phase IgM may be particularly important in opsonizing circulating ox-LDLs,[13] and perhaps also apoptotic cells and cell-derived microparticles, and in ensuring the robust disposal of such debris in safe locations. These protective functions of fluid-phase IgM may plausibly be mainly exerted in circulating plasma, liver, or spleen, whereas the accumulation of IgM on arterial lipid deposits activates proinflammatory functions in macrophages. Study of solid-phase immunoglobulins in plaque rupture *in vivo* will be technically challenging because most methods for analyzing ligand/receptor binding rely on a fluid-phase ligand. Moreover, a robust mouse model of plaque rupture has been lacking, related to the acknowledged substantial species difference between humans and mice.[54]

In conclusion, immunoglobulins activate macrophages more potently when in solid phase. In the case of IgG, this is mediated by the well-known CD16 pathway. In the case of IgM, this involves a novel IgM/SR-A pathway. Because activation by solid-phase immunoglobulins modulates key macrophage effector functions in plaque rupture and human ruptured plaques contain increased solid-phase immunoglobulin deposits, our data provide a novel insight into the pathophysiology of atherosclerotic plaque rupture.

References

1. Lewis MJ, Malik TH, Ehrenstein MR, Boyle JJ, Botto M, Haskard DO: Immunoglobulin M is required for protection against atherosclerosis in low-density lipoprotein receptor-deficient mice. Circulation 2009, 120:417–426
2. Kyaw T, Tay C, Khan A, Dumouchel V, Cao A, To K, Kehry M, Dunn R, Agrotis A, Tipping P, Bobik A, Toh BH: Conventional B2 B cell depletion ameliorates whereas its adoptive transfer aggravates atherosclerosis. J Immunol 2010, 185:4410–4419
3. Ravetch JV, Bolland S: IgG Fc receptors. Annu Rev Immunol 2001, 19:275–290
4. Aitman TJ, Dong R, Vyse TJ, Norsworthy PJ, Johnson MD, Smith J, Mangion J, Roberton-Lowe C, Marshall AJ, Petretto E, Hodges MD, Bhangal G, Patel SG, Sheehan-Rooney K, Duda M, Cook PR, Evans DJ, Domin J, Flint J, Boyle JJ, Pusey CD, Cook HT: Copy number polymorphism in Fcgr3 predisposes to glomerulonephritis in rats and humans. Nature 2006, 439:851–855
5. Boyle JJ: Human macrophages kill human mesangial cells by Fas-L-induced apoptosis when triggered by antibody via CD16. Clin Exp Immunol 2004, 137:529–537
6. Kelly JA, Griffin ME, Fava RA, Wood SG, Bessette KA, Miller ER, Huber SA, Binder CJ, Witztum JL, Morganelli PM. Inhibition of arterial lesion progression in CD16-deficient mice: evidence for altered immunity and the role of IL-10. Cardiovasc Res 2010, 85:224–231
7. Hartvigsen K, Chou MY, Hansen LF, Shaw PX, Tsimikas S, Binder CJ, Witztum JL. The role of innate immunity in atherogenesis. J Lipid Res 2009, 50(Suppl):S388–S393
8. Audard V, Georges B, Vanhille P, Toly C, Deroure B, Fakhouri F, Cuvelier R, Belenfant X, Surin B, Aucouturier P, Mougenot B, Ronco P: Renal lesions associated with IgM-secreting monoclonal

proliferations: revisiting the disease spectrum. Clin J Am Soc Nephrol 2008, 3:1339–1349
9. Carroll MC, Holers VM: Innate autoimmunity. Adv Immunol 2005, 86:137–157
10. Zhang M, Michael LH, Grosjean SA, Kelly RA, Carroll MC, Entman ML: The role of natural IgM in myocardial ischemia-reperfusion injury. J Mol Cell Cardiol 2006, 41:62–67
11. Kulik L, Fleming SD, Moratz C, Reuter JW, Novikov A, Chen K, Andrews KA, Markaryan A, Quigg RJ, Silverman GJ, Tsokos GC, Holers VM: Pathogenic natural antibodies recognizing annexin IV are required to develop intestinal ischemia-reperfusion injury. J Immunol 2009, 182:5363–5373
12. Shi T, Moulton VR, Lapchak PH, Deng GM, le Lucca JJ, Tsokos GC: Ischemia-mediated aggregation of the actin cytoskeleton is one of the major initial events resulting in ischemia-reperfusion injury. Am J Physiol Gastrointest Liver Physiol 2009, 296:G339–G347
13. Binder CJ, Shaw PX, Chang MK, Boullier A, Hartvigsen K, Horkko S, Miller YI, Woelkers DA, Corr M, Witztum JL: The role of natural antibodies in atherogenesis. J Lipid Res 2005, 46:1353–1363
14. Boyle JJ: Association of coronary plaque rupture and atherosclerotic inflammation. J Pathol 1997, 181:93–99
15. Horkko S, Bird DA, Miller E, Itabe H, Leitinger N, Subbanagounder G, Berliner JA, Friedman P, Dennis EA, Curtiss LK, Palinski W, Witztum JL: Monoclonal autoantibodies specific for oxidized phospholipids or oxidized phospholipid-protein adducts inhibit macrophage uptake of oxidized low-density lipoproteins. J Clin Invest 1999, 103:117–128
16. Kyaw T, Tay C, Krishnamurthi S, Kanellakis P, Agrotis A, Tipping P, Bobik A, Toh BH. B1a B lymphocytes are atheroprotective by secreting natural IgM that increases IgM deposits and reduces necrotic cores in atherosclerotic lesions. Circ Res 2011, 109:830–840
17. Shah PK: Molecular mechanisms of plaque instability. Curr Opin Lipidol 2007, 18:492–499
18. Littlewood TD, Bennett MR: Apoptotic cell death in atherosclerosis. Curr Opin Lipidol 2003, 14:469–475
19. de Winther MP, van Dijk KW, Havekes LM, Hofker MH: Macrophage scavenger receptor class A: a multifunctional receptor in atherosclerosis. Arterioscler Thromb Vasc Biol 2000, 20:290–297
20. Wung BS, Cheng JJ, Hsieh HJ, Shyy YJ, Wang DL: Cyclic strain-induced monocyte chemotactic protein-1 gene expression in endothelial cells involves reactive oxygen species activation of activator protein 1. Circ Res 1997, 81:1–7
21. Mietus-Snyder M, Friera A, Glass CK, Pitas RE: Regulation of scavenger receptor expression in smooth muscle cells by protein kinase C: a role for oxidative stress. Arterioscler Thromb Vasc Biol 1997, 17:969–978
22. Boyle JJ: Human macrophages kill human mesangial cells by Fas-L-induced apoptosis when triggered by antibody via CD16. Clin Exp Immunol 2004, 137:529–537
23. Lund I, Lundeberg T, Sandberg L, Budh CN, Kowalski J, Svensson E: Lack of interchangeability between visual analogue and verbal rating pain scales: a cross sectional description of pain etiology groups. BMC Med Res Methodol 2005, 5:31
24. Boyle JJ, Harrington HA, Piper E, Elderfield K, Stark J, Landis RC, Haskard DO: Coronary intraplaque hemorrhage evokes a novel atheroprotective macrophage phenotype. Am J Pathol 2009, 174: 1097–108
25. Aitman TJ, Dong R, Vyse TJ, Norsworthy PJ, Johnson MD, Smith J, Mangion J, Roberton-Lowe C, Marshall AJ, Petretto E, Hodges MD, Bhangal G, Patel SG, Sheehan-Rooney K, Duda M, Cook PR, Evans DJ, Domin J, Flint J, Boyle JJ, Pusey CD, Cook HT: Copy number polymorphism in Fcgr3 predisposes to glomerulonephritis in rats and humans. Nature 2006, 439:851–855
26. Cash JL, Hart R, Russ A, Dixon JP, Colledge WH, Doran J, Hendrick AG, Carlton MB, Greaves DR: Synthetic chemerin-derived peptides suppress inflammation through ChemR23. J Exp Med 2008, 205:767–775
27. Boyle JJ, Weissberg PL, Bennett MR: Human macrophage-induced vascular smooth muscle cell apoptosis requires NO enhancement of Fas/Fas-L interactions. Arterioscler Thromb Vasc Biol 2002, 22:1624–1630
28. Leung VW, Yun S, Botto M, Mason JC, Malik TH, Song W, Paixao-Cavalcante D, Pickering MC, Boyle JJ, Haskard DO: Decay-accelerating factor suppresses complement C3 activation and retards atherosclerosis in low-density lipoprotein receptor-deficient mice. Am J Pathol 2009, 175:1757–1767
29. Boyle JJ, Johns M, Kampfer T, Nguyen AT, Game L, Schaer DJ, Mason JC, Haskard DO. Activating Transcription Factor 1 directs Mhem atheroprotective macrophages via coordinated iron handling and foam cell protection. Circ Res 2012, (in press)
30. Boyle JJ, Bowyer DE, Weissberg PL, Bennett MR: Human blood-derived macrophages induce apoptosis in human plaque-derived vascular smooth muscle cells by Fas-ligand/Fas interactions. Arterioscler Thromb Vasc Biol 2001, 21:1402–1407
31. Boyle JJ, Weissberg PL, Bennett MR: Tumor necrosis factor-alpha promotes macrophage-induced vascular smooth muscle cell apoptosis by direct and autocrine mechanisms. Arterioscler Thromb Vasc Biol 2003, 23:1553–1558
32. Dai Y, Pei XY, Rahmani M, Conrad DH, Dent P, Grant S: Interruption of the NF-kappaB pathway by Bay 11–7082 promotes UCN-01-mediated mitochondrial dysfunction and apoptosis in human multiple myeloma cells. Blood 2004, 103:2761–2770
33. Hansson GK, Libby P: The immune response in atherosclerosis: a double-edged sword. Nat Rev Immunol 2006, 6:508–519
34. Hansson GK, Libby P, Schonbeck U, Yan ZQ: Innate and adaptive immunity in the pathogenesis of atherosclerosis. Circ Res 2002, 91:281–291
35. Naghavi M, Libby P, Falk E, Casscells SW, Litovsky S, Rumberger J, Badimon JJ, Stefanadis C, Moreno P, Pasterkamp G, Fayad Z, Stone PH, Waxman S, Raggi P, Madjid M, Zarrabi A, Burke A, Yuan C, Fitzgerald PJ, Siscovick DS, de Korte CL, Aikawa M, Juhani Airaksinen KE, Assmann G, Becker CR, Chesebro JH, Farb A, Galis ZS, Jackson C, Jang IK, Koenig W, Lodder RA, March K, Demirovic J, Navab M, Priori SG, Rekhter MD, Bahr R, Grundy SM, Mehran R, Colombo A, Boerwinkle E, Ballantyne C, Insull W, Jr., Schwartz RS, Vogel R, Serruys PW, Hansson GK, Faxon DP, Kaul S, Drexler H, Greenland P, Muller JE, Virmani R, Ridker PM, Zipes DP, Shah PK, Willerson JT: From vulnerable plaque to vulnerable patient: a call for new definitions and risk assessment strategies: part I. Circulation 2003, 108:1664–1672
36. Bjorkerud S, Bjorkerud B: Apoptosis is abundant in human atherosclerotic lesions, especially in inflammatory cells (macrophages and T cells), and may contribute to the accumulation of gruel and plaque instability. Am J Pathol 1996, 149:367–380
37. Greaves DR, Gordon S. The macrophage scavenger receptor at 30 years of age: current knowledge and future challenges. J Lipid Res 2009;50(Suppl):S282–S286
38. Chou MY, Fogelstrand L, Hartvigsen K, Hansen LF, Woelkers D, Shaw PX, Choi J, Perkmann T, Backhed F, Miller YI, Horkko S, Corr M, Witztum JL, Binder CJ: Oxidation-specific epitopes are dominant targets of innate natural antibodies in mice and humans. J Clin Invest 2009, 119:1335–1349
39. de Winther MP, Hofker MH: Scavenging new insights into atherogenesis. J Clin Invest 2000, 105:1039–1041
40. Witztum JL. You are right too! J Clin Invest 2005, 115:2072–2075
41. Kirkham PA, Spooner G, Ffoulkes-Jones C, Calvez R: Cigarette smoke triggers macrophage adhesion and activation: role of lipid peroxidation products and scavenger receptor. Free Radic Biol Med 2003, 35:697–710
42. Platt N, Gordon S: Is the class A macrophage scavenger receptor (SR-A) multifunctional? - the mouse's tale. J Clin Invest 2001, 108: 649–654
43. Guicciardi ME, Gores GJ: Life and death by death receptors. FASEB J 2009, 23:1625–1637
44. Werb Z, Takemura R, Stenberg PE, Bainton DF: Directed exocytosis of secretory granules containing apolipoprotein E to the adherent surface and basal vacuoles of macrophages spreading on immobile immune complexes. Am J Pathol 1989, 134:661–670
45. Schwartz SM, Virmani R, Rosenfeld ME: The good smooth muscle cells in atherosclerosis. Curr Atheroscler Rep 2000, 2:422–429
46. Imanishi T, Han DK, Hofstra L, Hano T, Nishio I, Liles WC, Gown AM, Schwartz SM: Apoptosis of vascular smooth muscle cells is induced by Fas ligand derived from monocytes/macrophage. Atherosclerosis 2002, 161:143–151
47. Vasudevan SS, Lopes NH, Seshiah PN, Wang T, Marsh CB, Kereiakes DJ, Dong C, Goldschmidt-Clermont PJ: Mac-1 and Fas activities are concurrently required for execution of smooth muscle cell

death by M-CSF-stimulated macrophages. Cardiovasc Res 2003, 59:723–733
48. Hansson GK, Bondjers G, Nilsson LA: Plasma protein accumulation in injured endothelial cells. Immunofluorescent localization of IgG and fibrinogen in the rabbit aortic endothelium. Exp Mol Pathol 1979, 30:12–26
49. Hansson GK, Bondjers G, Bylock A, Hjalmarsson L: Ultrastructural studies on the localization of IgG in the aortic endothelium and subendothelial intima of atherosclerotic and nonatherosclerotic rabbits. Exp Mol Pathol 1980, 33:302–315
50. Hansson GK, Holm J, Kral JG: Accumulation of IgG and complement factor C3 in human arterial endothelium and atherosclerotic lesions. Acta Pathol Microbiol Immunol Scand A 1984, 92:429–435
51. Seifert PS, Hansson GK: Complement receptors and regulatory proteins in human atherosclerotic lesions. Arteriosclerosis 1989, 9:802–811
52. Naghavi M, Libby P, Falk E, Casscells SW, Litovsky S, Rumberger J, Badimon JJ, Stefanadis C, Moreno P, Pasterkamp G, Fayad Z, Stone PH, Waxman S, Raggi P, Madjid M, Zarrabi A, Burke A, Yuan C, Fitzgerald PJ, Siscovick DS, de Korte CL, Aikawa M, Airaksinen KE, Assmann G, Becker CR, Chesebro JH, Farb A, Galis ZS, Jackson C, Jang IK, Koenig W, Lodder RA, March K, Demirovic J, Navab M, Priori SG, Rekhter MD, Bahr R, Grundy SM, Mehran R, Colombo A, Boerwinkle E, Ballantyne C, Insull W, Jr., Schwartz RS, Vogel R, Serruys PW, Hansson GK, Faxon DP, Kaul S, Drexler H, Greenland P, Muller JE, Virmani R, Ridker PM, Zipes DP, Shah PK, Willerson JT: From vulnerable plaque to vulnerable patient: a call for new definitions and risk assessment strategies: part II. Circulation 2003, 108: 1772–1778
53. Kramer MC, van der Wal AC, Koch KT, Rittersma SZ, Li X, Ploegmakers HP, Henriques JP, Van der Schaaf RJ, Baan J, Jr., Vis MM, Meesterman MG, Piek JJ, Tijssen JG, De Winter RJ: Histopathological features of aspirated thrombi after primary percutaneous coronary intervention in patients with ST-elevation myocardial infarction. PLoS ONE 2009, 4:e5817
54. Bennett MR: Breaking the plaque: evidence for plaque rupture in animal models of atherosclerosis. Arterioscler Thromb Vasc Biol 2002, 22:713–714